L-subshell ionization cross sections in gold and bismuth by 3.6–9.5-MeV carbon and 4.0–7.2-MeV oxygen ions

D. Bhattacharya, M. Sarkar, M. B. Chatterjee, and P. Sen
Saha Institute of Nuclear Physics, 1/AF Bidhannagar, Calcutta 700064, India

G. Kuri and D. P. Mahapatra
Institute of Physics, Sachivalaya Marg, Bhubaneswar, Orissa 751005, India

G. Lapicki
Department of Physics, East Carolina University, Greenville, North Carolina 27858
(Received 27 January 1994)

L-subshell ionization cross sections of Au and Bi induced by $C^{2,3+}$ and O^{3+} ions have been measured for impact energies ranging from 0.25 to 0.79 MeV/u. The data have been compared with the predictions of the ECPSSR [perturbed-stationary-state (PSS) theory with energy-loss (E), Coulomb deflection (C), and relativistic corrections (R)] theory. Reasonable agreement between theory and experiment is observed for the $L_1(2s_{1/2})$ and $L_3(2p_{3/2})$ subshells. For the $L_2(2p_{1/2})$ subshell, however, large disagreement between the data and the ECPSSR predictions persists. This difference could be due to the "collision-induced intrashell" mechanism that was suggested by Sarkadi and Mukoyama [J. Phys. B **14**, L255 (1981)].

PACS number(s): 34.50.Fa

I. INTRODUCTION

A quick look into the x-ray cross-section data published so far [1–7] reveals that a large portion of these are on K and L shells ionized by protons or α particles. This could be due to the fact that in routine particle-induced x-ray emission (PIXE) analysis, K- and L-shell ionization cross sections induced by protons or helium ions are being used. Cross sections induced by heavy ions (other than helium) are comparatively scanty, particularly so for L-shell ionization. Table I surveys the published data on L-shell ionization by heavy ions after 1975 [8–20].

To understand the mechanism of inner-shell ionization in ion-atom collisions, several theories such as plane-wave born approximation (PWBA) [21], binary-encounter approximation (BEA) [22,23], and semiclassical approximation (SCA) [24] have been formulated. Corrections due to the projectile energy loss (E), coulomb deflection of the projectile in the field of the target nucleus (C), relativistic nature of the inner-shell electrons (R), and polarization and increased binding of the inner-shell electrons have been introduced into the PWBA formalism through perturbed-stationary-state (PSS) [25] calculation, which is known and abbreviated as ECPSSR. In PIXE work, the ECPSSR theory has received wide acceptance and comparison of the predictions of this theory with the experimental data on K-shell ionization are also generally satis-

TABLE I. A survey of heavy-ion induced L-shell ionization data after 1975.

Projectile	Target	Energy range (MeV)	Reference
C,O	Ta,Au,Bi,U	6–96	Li, Clark, and Greenless [8]
C,N,O	Au	0.4–3.4	Sarkadi and Mukoyama [9]
F	Si,S,Ar,Kr	1–25	Presser, Scherer, and Stähler [10]
N	Au	3.0–18.2	Pàlinkàs *et al.* [11]
Li,Be,C,O,Ne,Si,S	Au	1.6–107.2	Jitschin *et al.*, [12]
C,N	Sm,Er,Au	2.4–2.8	Papp *et al.* [13]
Si,S	Au	7.0–80.2	Berinde *et al.* [14]
Ag	Yb,Tb,W,Pt,Pb, Th	107.9	Uchai *et al.* [15]
C,O	In,Nd,Gd,Ho,Tb, Au,Pb	25,32	Andrews *et al.* [16]
O,Ne	Bi	10,20,88	Ito *et al.* [17]
Li	Eu,Gd,Dy,Ho	2.2–4.50	Xiaohong *et al.* [18]
Li	Ca,Fe,Ni,Cu,Ge	0.75–4.5	McNeir *et al.* [19]
C	Cu,Ga,Ge,Br,Y,Nd, Gd,Ho,Yb,Au,Pb	2–25	Mehta *et al.* [20]

factory [5,6].

Unlike the K shell, the L shell has three subshells, all with different properties. Thus to test the validity of the theoretical models in a stringent manner, some groups have chosen the L subshells as their subject of investigation. It has been reported by several groups [26–33,39] that even in the case of proton or helium impact, although $L_1(2s_{1/2})$ and $L_3(2p_{3/2})$ ionization cross sections agree well with the ECPSSR theory, it fails to reproduce the $L_2(2p_{1/2})$ cross section by almost an order of magnitude. This effect is also reflected in the ratios of the line intensities arising from the respective L subshells. Early in the last decade, Sarkadi and Mukoyama [33] suggested that this mismatch could be due to "collision-induced intra-shell transition" (subshell coupling) occurring during the L-shell ionization. Later in 1988 [34], they used the relativistic plane-wave born approximation (RPWBA) with Dirac-Hartree-Slater (DHS) wave functions including the binding (B) and coulomb (C) corrections (RPWBA-DHS-BC). Main features of the data were reproduced when Sarkadi and Mukoyama combined these calculations with their subshell coupling scheme, although a deviation of about 35% between experiment and theory remained. Vigilante *et al.* [30] have modified the binding correction and made a united-atom-ECPSSR recalculation for proton and helium ions for some elements. Even after introducing the subshell coupling, the L-subshell discrepancy could not be removed. Cohen [35] in his review paper suggested that the cause of this discrepancy might possibly derive from (i) subshell coupling (as suggested by Sarkadi and Mukoyama [33]) and (ii) improper choice of values of the parameters, such as fluorescence yields (ω_i), Coster-Kronig yields (f_{ij}), and radiative widths (Γ) that are used to convert the experimental cross sections to ionization cross sections. Recently Xu [36] has analyzed proton-induced Au L-shell data from the literature and, using his prescribed set of ω_i and f_{ij} values, has shown that in the energy range 0.18–10 MeV the experimental data and theoretical predictions of ECPSSR are in excellent agreement with each other. Xu did not observe any influence of the subshell coupling effect (or, it was too weak to be found). In a subsequent paper [37], by analyzing the data of Pb and Bi, Xu and Xu drew similar conclusions.

The situation is thus rather ambiguous. It is very difficult to decipher whether intra-shell coupling effect or the lack of accurate values for the x-ray-to-ionization conversion factors is actually responsible for the disagreement between the experiment and theory. Sarkadi and Mukoyama [33] argued that their proposed intra-shell coupling effect would be large at lower incident energy and high atomic number Z_1 of the projectile, i.e., at low projectile velocity relative to the electron velocity in the L-shell orbit $v_{2L}=(Z_2-4.15)v_0/2$ (v_0 is the Bohr velocity) and when the Z_1-to-Z_2 ratio is not too small. Aiming at a resolution of this ambiguity, we decided to undertake the present investigation of the L-subshell ionization of Au and Bi in collision with carbon and oxygen beams in the energy range 3.6–9.5 MeV. This allows us to probe the role of the intra-shell coupling at v_1/v_{2L} as low as 0.08 and with a Z_1-to-Z_2 ratio as large as 0.1. Moreover, all of our measurements reported here will be an addition to the existing data bank. Since Au has already been used as the proverbial gold standard by different groups to investigate the controversial situation mentioned above, we have deliberately chosen Au as one of our targets.

II. EXPERIMENTAL PROCEDURE

The experiment was performed with a 3-MV 9SDH-2 tandem Pelletron at the Institute of Physics, Bhubaneswar, Orissa, India. C^{2+}, C^{3+}, and O^{3+} projectiles were used in the energy range of 0.25–0.79 MeV/u. After the analyzing and switching magnets the beam was collimated through an aperture of 2 mm before entering the scattering chamber. The vacuum inside the chamber was kept at 2×10^{-6} torr. Au and Bi targets of ≈100 and ≈200 $\mu g/cm^2$, respectively, were vacuum deposited on ≈15 $\mu g/cm^2$ carbon backing. Targets were placed at an angle of 45° to the beam. L x rays were detected at 90° with a Si(Li) detector having a resolution of ≈180 eV at 5.9 keV. The beam spot size at the target position was about 2 mm in diameter as observed from the mark left by the beam on a paper target. The scattering chamber had a 12.7-μm-thick Be window through which the Si(Li) detector saw the x rays. To cut down the copious M x rays, a 40-μm Al foil was placed in front of the detector window. The count rate was always maintained at less than 1000 counts/s to avoid the necessity of any dead-time correction. During the measurement the energy calibration was checked with ^{57}Co and ^{241}Am sources and a maximum drift of 5 eV was found. A surface-barrier detector was placed at an angle of 152° to the beam to detect the backscattered particles. Simultaneous measurement of the scattered particles and the x rays helps to normalize the x-ray data and check the target condition on line. The solid angle subtended by the surface-barrier detector at the target was 1.24×10^{-3} sr. A typical spectrum of Bi L x rays bombarded by 4.8-MeV C^{3+} ions is shown in Fig. 1. The time required to acquire a meaningful spectrum varied from 15 min to 2 h. The beam

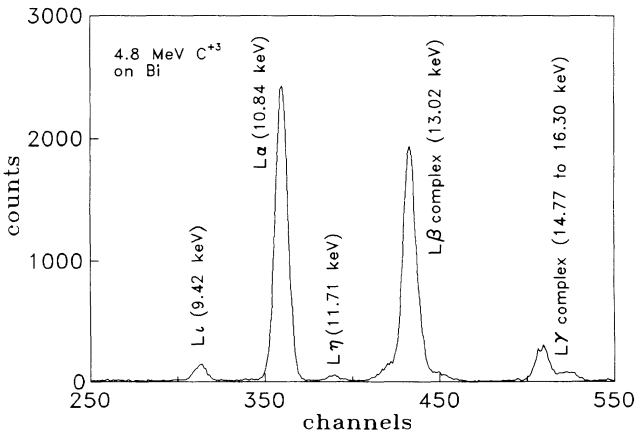

FIG. 1. L x-ray spectrum of bismuth bombarded by 4.8-MeV C^{3+} ions.

current during the run was between 10–50 nA. The efficiency of the Si(Li) detector was measured using calibrated sources of ^{241}Am, ^{57}Co, and ^{133}Ba. The overall error in the efficiency measurement was 10% in our energy range of interest.

III. DATA ANALYSIS AND RESULTS

The single lines of the x-ray spectra, e.g., Ll, $L\alpha$, and $L\eta$ were fitted to single Gaussians with a linear background. The $L\gamma$ complex was fitted to four Gaussians. Using the relation (1),

$$\sigma_p^x = \frac{\sigma^R(\theta)(d\Omega)_p N_x}{N_p \varepsilon'} F \ , \tag{1}$$

x-ray production cross sections of all the resolved lines were calculated where $\sigma^R(\theta)$ is the Rutherford cross section at an angle θ, $(d\Omega)_p$ is the solid angle subtended by the particle detector, N_x is the peak integral of the x-ray line, N_p is the peak integral of the elastically scattered projectiles, ε' is the effective efficiency of the Si(Li) detector (including the solid angle and the absorption of x rays in the aluminum absorber), and F is the correction factor for target thickness and anisotropic emission of x rays.

A. Corrections for target thickness

This correction factor arises due to two reasons: (a) the slowing down of the projectile inside the target, which means that the x-ray ionization cross section is changing, and (b) the self-absorption of the x rays inside the target. Both of these factors are taken care of by Laubert *et al.* [38] and Papp *et al.* [39]. In our case we followed the method of Laubert *et al.*, although both methods give very similar results. The maximum increase in cross section due to this factor is 39% for the Ll line of Bi in 4.8-MeV C-ion impact and the minimum increase is 6% for the $L\gamma_{44'}$ line of Au in 9.5-MeV C-ion impact.

B. Correction for the vacancy alignment

It has been pointed out by several authors [40–42] that the collision will induce alignment of vacancies in the subshells of the target with angular momentum $j > \frac{1}{2}$. This alignment is then reflected in the anisotropic emission of the x rays or auger electrons from that particular subshell. In our case, Ll, $L\alpha$, and $L\beta_{2,15}$ lines will be affected. Corrections to the intensities of the above lines have been made using the experimental values of the alignment parameters of Jitschin *et al.* [42]. The maximum effect of the alignment was on the Ll line of Au in the O^{3+} collision, where intensity had been lowered by 11% in our energy range. However, the intensity of the lines ($L\alpha$, $L\gamma_1$, and $L\gamma_{2,3,6}$) that actually determine the extracted cross sections are either unaffected (such as for $L\gamma_1$ and $L\gamma_{2,3,6}$) or decreased by a maximum of 1% (for $L\alpha$) by this effect. As there is no experimental alignment data on Bi, we took the same values as that of Au, assuming that this effect will not vary much between Au and Bi.

The lines that could be resolved in the present analysis are Ll, $L\alpha$, $L\eta$, $L\beta$, $L\gamma_5$, $L\gamma_1$, $L\gamma_{2,3,6}$ and $L\gamma_{44'}$. The two corrections, as mentioned above, are incorporated and the absolute values of the x-ray production cross sections of the above lines obtained using relation (1) are shown in Table II.

In order to get the subshell ionization cross sections, we followed the method of Datz *et al.* [43]. First, the intensity of the $\gamma_{2,3}$ line was obtained from the line intensities of $\gamma_{2,3,6}$ and γ_1 using the intensity ratio of γ_6 and γ_1 lines from Campbell and Wang [44]. From the x-ray production cross sections of $\gamma_{2,3}$, γ_1, and α lines, the ionization cross sections of L_1, L_2, and L_3 subshells were calculated using the various fluorescence, Coster-Kronig yields, and radiative transition rates. We tried a number of sets for fluorescence and Coster-Kronig yields, ω_i and f_{ij}: for Au, two sets were from Sarkadi and Mukoyama [9] and one set from Xu [36], and for Bi one set was from Xu and Xu [37] and another from Krause [45]. The radi-

TABLE II. Experimental x-ray production cross sections (mb) of the different L lines. Errors are ≈30%.

Projectile	E (MeV)	Ll	$L\alpha$	$L\eta$	$L\beta$	$L\gamma_5$	$L\gamma_1$	$L\gamma_{236}$	$L\gamma_{44'}$
				Au					
C^{2+}	3.6	32.2	495.3	8.6	470.8	3.0	62.5	21.0	2.8
C^{3+}	4.8	148.6	2 349.6	34.4	1 864.4	11.0	232.8	79.3	12.7
	7.2	602.3	9 210.7	72.8	6 010.5	31.5	757.6	207.8	23.9
	9.5	1249.4	21 139.5	251.0	12 679.4	60.2	1452.9	442.1	41.4
				Au					
O^{3+}	4.0	18.5	355.9	10.0	443.7	2.9	68.3	16.2	1.0
	5.6	79.2	1 445.1	27.7	1 394.5	7.1	199.8	52.9	5.4
	7.2	295.8	4 945.5	74.0	3 939.0	22.7	519.7	131.8	13.8
				Bi					
C^{3+}	4.8	97.3	1 680.8	24.5	1 241.7	7.0	176.1	54.0	7.3
	7.2	367.8	6 011.5	68.6	3 576.7	34.7	473.4	143.9	24.7
	9.5	827.2	14 233.6	126.9	7 887.9	62.0	969.9	270.9	33.4

ative transition rates in both Au and Bi are from Campbell and Wang [44]. Table III shows all the parameters used in the conversion of x-ray production cross sections to ionization data. Since extracted ionization cross sections were within experimental uncertainties independent of the set of conversion factors chosen, only Xu's values were used to draw these cross sections in Fig. 2 for comparison with the ECPSSR theory. Figure 3 exhibits the σ_1/σ_2, σ_1/σ_3, and σ_2/σ_3 ratios, comparing our values with the predictions of the ECPSSR theory as well as with the measurements of other groups.

IV. DISCUSSION

In the 3.6–9.5-MeV energy range, there are no data to compare with our experimental data shown in Table II. Jitschin *et al.* [12] published only the intensity ratio of the lines $L\alpha$, $L\gamma_1$, and $L\gamma_{2,3,6}$ in bombardment of Au by C and O ions. Their values agree with ours within experimental uncertainties; the ECPSSR calculations are lower by about 50–100%, the gap increasing with decreasing ion energy. The data of Sarkadi and Mukoyama [9] on Au are almost exclusively below our energy range; their

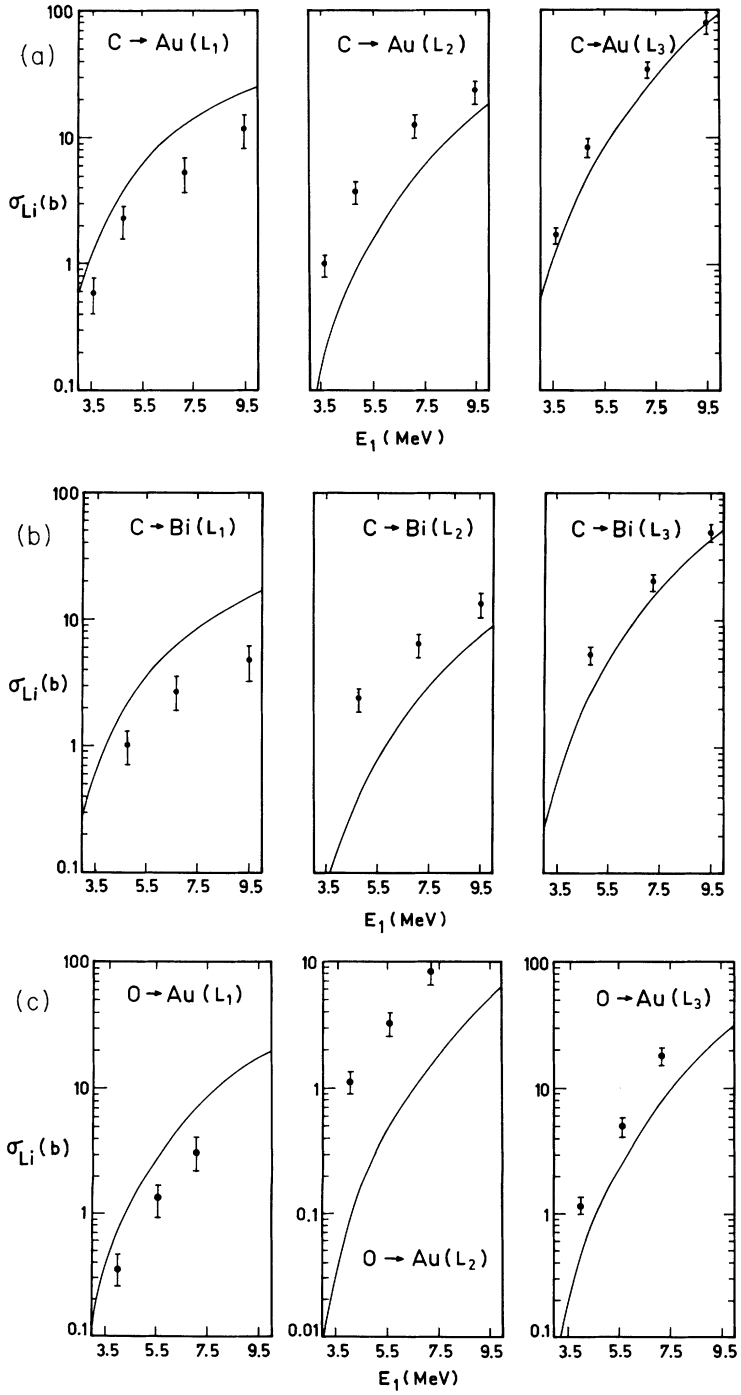

FIG. 2. (a) L-subshell ionization cross sections (in barn) of gold by carbon ions. ●, this work; ——, ECPSSR. (b) L-subshell ionization cross sections (in barn) of bismuth by carbon ions. ●, this work; ——, ECPSSR. (c) L-subshell ionization cross sections (in barns) of gold by oxygen ions. ●, this work; ——, ECPSSR.

TABLE III. Various sets of parameters used to convert x-ray production cross sections to ionization cross sections.

	Au			Bi	
	Sarkadi and Mukoyama Ref. [9]		Xu Ref. [36]	Xu and Xu Ref. [37]	Krause Ref. [45]
ω_1	0.105	0.107	0.121	0.138	0.117
ω_2	0.357	0.334	0.355	0.428	0.387
ω_3	0.327	0.320	0.296	0.340	0.373
f_{12}	0.083	0.140	0.120	0.0549	0.11
f_{13}	0.644	0.530	0.56	0.70	0.58
f_{23}	0.132	0.122	0.12	0.12	0.113
Γ_1	1.0968	1.0968	1.0968	1.403	1.403
Γ_2	1.9942	1.9942	1.9942	2.5689	2.5689
Γ_3	1.7444	1.7444	1.7444	2.216	2.216
$\Gamma_{\gamma_6}/\Gamma_{\gamma_1}$	0.1056	0.1056	0.1056	0.1443	0.1443
$\Gamma_{\gamma_{2,3}}$	0.2196	0.2196	0.2196	0.283	0.283
Γ_{γ_1}	0.3288	0.3288	0.3288	0.4336	0.4336
Γ_α	1.3599	1.3599	1.3599	1.701	1.701

highest energy overlaps with ours for carbon ions and their $L\alpha$ ionization cross section is in good agreement with our measurement, as shown in Fig. 4. Given that $L\alpha$ x rays originate exclusively from the vacancy in the L_3 subshell, this agreement could be easily anticipated from Fig. 2, where the L_3-subshell cross sections are in very good agreement with the ECPSSR theory. By contrast, $L\gamma$ x rays, whose production depends on the L_1 and L_2 subshells, which as seen in Fig. 2 are poorly described by the ECPSSR, are in poor agreement with the theory as illustrated in Fig. 5 for the $L\gamma_1$-to-$L\alpha$ and $L\gamma_{2,3,6}$-to-$L\alpha$ ratios.

Krause's [45] fluorescence and Coster-Kronig yields were employed in Fig. 6. Xu *et al.* [36,37] claimed that—with some adjustment of these yields—the intensity ratios of I_α/I_β and I_α/I_γ in proton- and helium-induced ionization could be exactly reproduced by the ECPSSR. The intensity ratios for these lines induced in heavy-ion collisions of our present experiment are indeed in better agreement with the ECPSSR when Xu's [36] in-

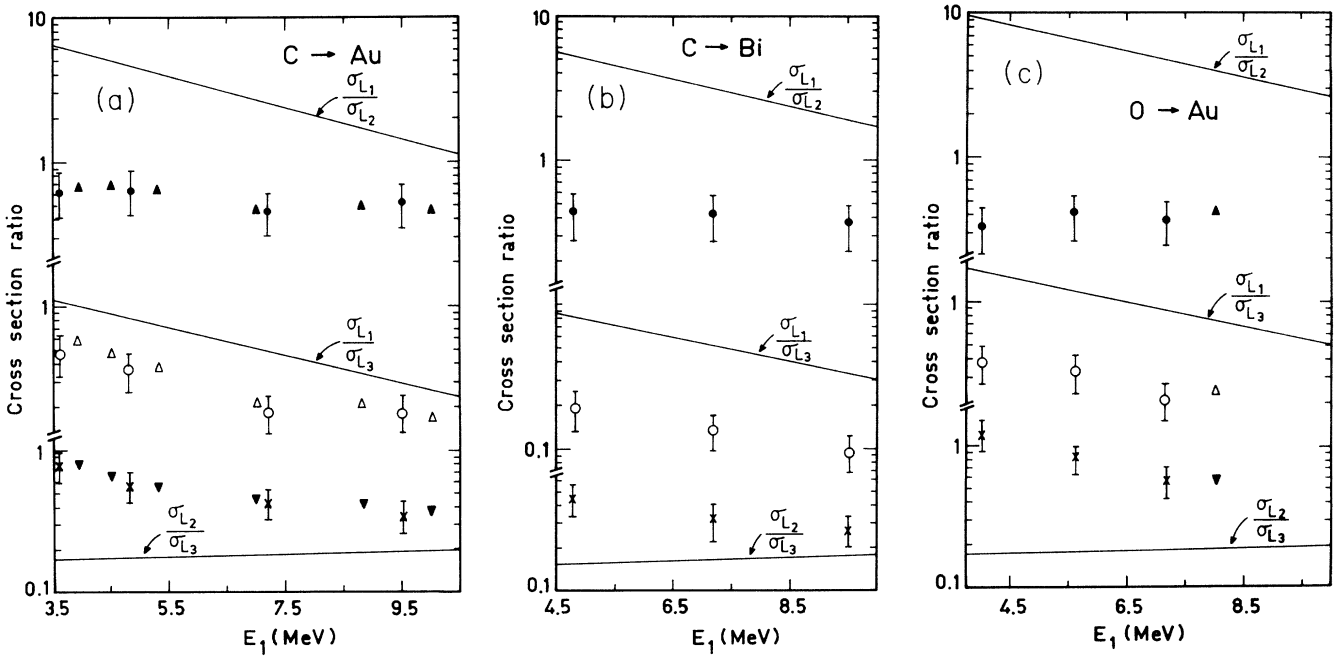

FIG. 3. (a) L-subshell ionization cross-section ratios in gold by carbon ions. For $\sigma_{L_1}/\sigma_{L_2}$: ●, this work; ▲, Jitschin *et al.* [12]. For $\sigma_{L_1}/\sigma_{L_3}$: ○, this work; △, Jitschin *et al.* [12]. For $\sigma_{L_2}/\sigma_{L_3}$: ×, this work; ▼, Jitschin *et al.* [12]; ——, ECPSSR. (b) L-subshell ionization cross-section ratios in bismuth by carbon ions. Symbols are same as (a). (c) L-subshell ionization cross-section ratios in gold by oxygen ions. Symbols are same as (a).

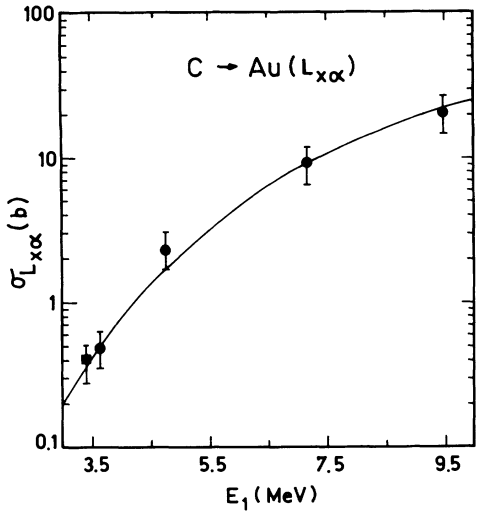

FIG. 4. L_α x-ray production cross sections (in barn) in gold by carbon ions. ●, this work; ■, Sarkadi and Mukoyama [9]; ——, ECPSSR.

stead of Krause's [45] yields are chosen. However, as seen in Fig. 6, the ECPSSR still deviates by as much as two standard deviations from our data. Although these deviations subside with increasing energy, the large disagreement at the lowest energies mirrors the discrepancies for individual subshell ionization cross sections, as demonstrated in Fig. 2 and discussed below.

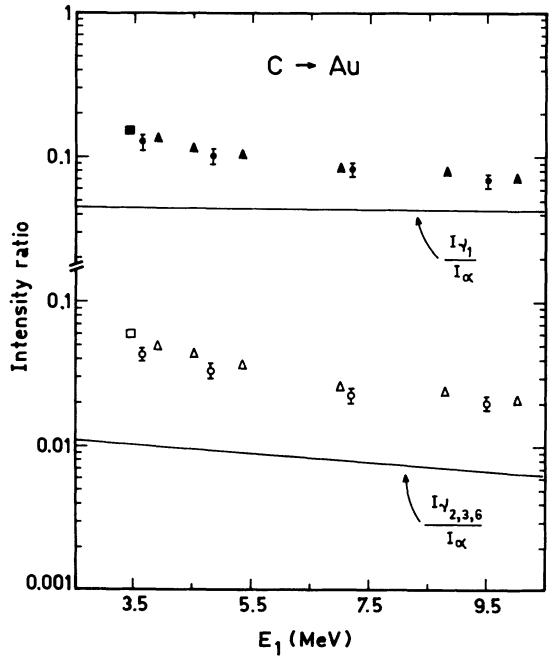

FIG. 5. Intensity ratios for x-ray production I_{γ_1}/I_α and $I_{\gamma_{2,3,6}}/I_\alpha$ gold by carbon ions. For I_{γ_1}/I_α: ●, this work; ■, Sarkadi and Mukoyama [9]; ▲, Jitschin *et al.* [12]. For $I_{\gamma_{2,3,6}}/I_\alpha$: ○, this work; □, Sarkadi and Mukoyama [9]; △, Jitschin *et al.* [12]; ——, ECPSSR.

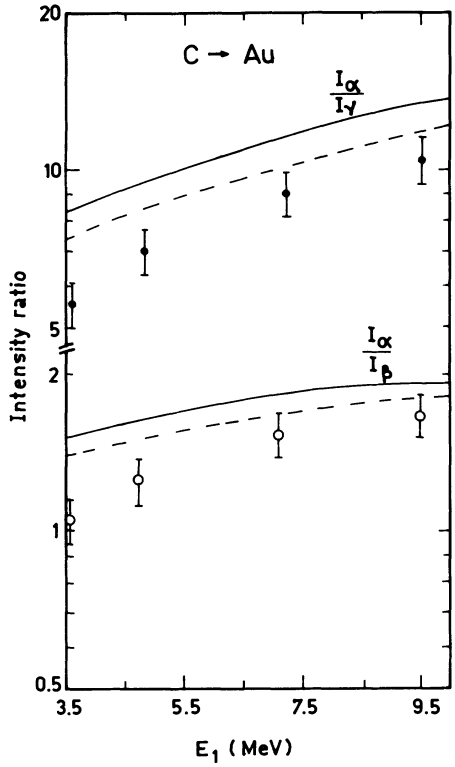

FIG. 6. Intensity ratios for x-ray production I_α/I_γ and I_α/I_β in gold by carbon ion. For I_α/I_γ: ●, this work. For I_α/I_β: ○, this work; ——, ECPSSR (Krause); — — —, ECPSSR (Xu).

In Fig. 2, L_1-subshell ionization cross sections in Au and Bi lie below the predictions of the ECPSSR theory; our data are some 30–50 % lower than these predictions. This is contrary to what is seen for L_2 and L_3 ionization. For L_3, the ECPSSR is in reasonable agreement with our carbon data, although for oxygen ions it falls 20% below the measurements. The pronounced and known discrepancies between the ECPSSR and the data for the L_2 subshell are clearly evident in Fig. 2; for C ions the ECPSSR is a factor of 2–3 below our measurements and lower by as much as a factor of 10 for ionization by O ions.

To reduce the systematic errors that might have afflicted the extracted ionization cross sections, it is often preferable to consider their ratios. As seen in Fig. 3, our σ_{L_1}-to-σ_{L_2}, σ_{L_1}-to-σ_{L_3}, and σ_{L_2}-to-σ_{L_3} ratios are consistent with those of Jitschin *et al.* [12]. The ECPSSR manifestly fails to predict these ratios. This failure becomes especially pronounced at lower energies.

As reported previously [46], multiple ionization occurs in our present collision system. The peak position of the $L\alpha$ line is shifted by about 30 eV relative to its location in proton bombardment. As pointed out by Jitschin *et al.* [12] such a shift corresponds to the creation of one hole in the M shell and a number of holes in higher shells. This could increase ω_1 by almost a factor of 2, thereby reducing σ_{L_1}. In contrast, the ω_2 and ω_3 values are not

affected much by multiple ionization of the outer shells. Hence σ_{L_2}-to-σ_{L_3} is even less dependent on multiple ionization, remaining—in particular at lower energies—always higher than the ECPSSR calculations.

Such anomalous behavior cannot be explained using an enhanced ω_1, as this would result in smaller σ_{L_1} and thus worsen the agreement between theory and experiment even further. It appears that the only explanation of this anamoly was given by Sarkadi and Mukayama [33] where they proposed the so-called "collision-induced intra-shell transition" to account for the observed discrepancies. They noted that these transitions became more important with the decreasing energy and increasing atomic number of the projectile. This idea was further supported by Finck, Jitschin, and Lutz [47] and Cohen [35]. In the present work, the deviations are indeed more substantial at lowest energies and for O ions. Work on ion-induced intra-shell transition is in progress and it will be reported in the near future.

V. CONCLUSION

The following are the main outcomes of the present analysis:

(i) For the first time, x-ray production cross sections are reported for different L lines of Au and Bi bombarded by C and O ions at such low energies.

(ii) The disagreement between our data and the ECPSSR predictions cannot be removed with a mere adjustment of fluorescence yields for our collision systems.

(iii) The so-called collision-induced intra-shell transition mechanism [33] remains a viable explanation for these discrepancies.

ACKNOWLEDGMENT

The authors thank the crew of the pelletron machine for providing the various ion beams.

[1] C. H. Rutledge and R. L. Watson, At. Data Nucl. Data Tables **12**, 195 (1973).
[2] I. L. Hardt and R. L. Watson, At. Data Nucl. Tables **17**, 107 (1976).
[3] R. K. Gardner and T. G. Gray, At. Data Nucl. Data Tables **21**, 515 (1978); **24**, 281 (1979).
[4] H. Paul, At. Data Nucl. Data Tables **24**, 243 (1978).
[5] R. S. Sokhi and D. Crumpton, At. Data Nucl. Data Tables **30**, 49 (1984).
[6] H. Paul and J. Muhr, Phys. Rep. **135**, 47 (1986).
[7] G. Lapicki, J. Phys. Chem. Ref. Data **18**, 111 (1989).
[8] T. K. Li, D. L. Clark, and W. Greenless, Phys. Rev. Lett. **37**, 1209 (1976).
[9] L. Sarkadi and T. Mukoyama, J. Phys. B **13**, 2255 (1980).
[10] G. Presser, E. Scherer, and J. Stähler, Z. Phys. **295**, 27 (1980).
[11] J. Pàlinkàs, L. Sarkadi, B. Schlenk, I. Török, G. Kàlmàn, C. Bauer, K. Brankoff, D. Grambole, C. Heiser, W. Rudolph, and H. J. Thomas, J. Phys. B **17**, 131 (1983).
[12] W. Jitschin, R. Hippler, K. Finck, R. Schuch, and H. O. Lutz, J. Phys. B **16**, 4405 (1983).
[13] T. Papp, J. Pàlinkàs, L. Sarkadi, B. Schlenk, I. Török, and K. Kiss, Nucl. Instrum. Methods Phys. Res. Sect. B **4**, 311 (1984).
[14] A. Berinde, C. Ciortea, Al. Enulescu, D. Fluerasu, I. Piticu, V. Zoran, and D. Trautmann, Nucl. Instrum. Methods Phys. Res. Sect. B **4**, 283 (1984).
[15] W. Uchai, G. Lapicki, W. T. Milner, S. Raman, P. V. Rao, and C. R. Vane, J. Phys. B **18**, L389 (1985).
[16] M. C. Andrews, F. D. Mcdaniel, J. L. Duggan, P. D. Miller, P. L. Pepmiller, H. F. Krause, T. M. Rosseel, L. A. Rayburn, R. Mehta, and G. Lapicki, Nucl. Instrum. Methods Phys. Res. Sect. B **10/11**, 181 (1985); Phys. Rev. A **36**, 3699 (1987).
[17] S. Ito, M. Shoji, N. Maeda, R. Katano, T. Mukoyama, R. Ono, and Y. Nakayama, J. Phys. B **20**, L597 (1987).
[18] C. Xiaohong, L. Jihu, L. Zhaoyuan, M. Shuxun, and D. Fayun, Vacuum **39**, 393 (1989).
[19] M. R. McNeir, Y. C. Yu, D. L. Weathers, D. K. Marble, J. L. Duggan, and E. D. McDaniel, Nucl. Instrum. Methods Phys. Res. Sect. B **56/57**, 26 (1991).
[20] R. Mehta, J. L. Duggan, F. D. Mcdaniel, M. R. McNeir, Y. C. Yu, D. K. Marble, and G. Lapicki, Nucl. Instrum. Methods Phys. Res. Sect. B **79**, 175 (1993).
[21] E. Merzbacher and L. W. Lewis, in *X-ray Production by Heavy Charged Particles,* edited by S. Flugge, Encyclopedia of Physics Vol. 34 (Springer, Berlin, 1958).
[22] J. D. Garcia, Phys. Rev. A **1**, 280 (1970).
[23] J. S. Hansen, Phys. Rev. A **8**, 822 (1973).
[24] J. Bang and J. M. Hansteen, K. Dan. Vidensk. Selsk. Mat. Fys. Medd. **31**, 13 (1959); J. M. Hansteen and O. P. Mosebekk, Z. Phys. **234**, 281 (1970).
[25] W. Brandt and G. Lapicki, Phys. Rev. A **23**, 1717 (1981).
[26] W. Jischin, A. Kaschuba, R. Hippler, and H. O. Lutz, J. Phys. B **15**, 763 (1982).
[27] D. Cohen and M. Harrigan, At. Data Nucl. Data Tables **34**, 393 (1986).
[28] L. Sarkadi and T. Mukoyama, Nucl. Instrum. Methods Phys. Res. Sect. B **4**, 296 (1984); T. Mukoyama and L. Sarkadi, Nucl. Instrum. Methods **190**, 619 (1981); **205**, 341 (1983); **211**, 525 (1983).
[29] D. Cohen, Nucl. Instrum. Methods **218**, 795 (1983); Nucl. Instrum. Methods Phys. Res. Sect. B **3**, 47 (1984); **49**, 1 (1990); D. Cohen and M. Harrigan, *ibid.* **15**, 576 (1986).
[30] M. Vigilante, P. Cuzzocrea, N. De. Cesare, F. Murolo, E. Perillo, and G. Spadaccini, Nucl. Instrum. Methods Phys. Res. Sect. B **51**, 232 (1990).
[31] J. Braziewicz, M. Pajek, E. Braziewicz, J. Ploskonka, and G. M. Osetynski, Nucl. Instrum. Methods Phys. Res. Sect. B **15**, 585 (1986).
[32] M. H. Chen, B. Crasemann, and H. Mark, Phys. Rev. A **26**, 1243 (1982).
[33] L. Sarkadi and T. Mukoyama, J. Phys. B **14**, L255 (1981).
[34] L. Sarkadi and T. Mukoyama, Phys. Rev. A **37**, 4540 (1988).
[35] D. Cohen, Nucl. Instrum. Methods Phys. Res. Sect. B **49**, 1 (1990).
[36] J. Q. Xu, Phys. Rev. A **44**, 373 (1991).
[37] J. Q. Xu and X. J. Xu, J. Phys. B **25**, 695 (1992).
[38] R. Laubert, H. Haselton, J. R. Mowat, R. S. Peterson, and

I. A. Sellin, Phys. Rev. A **11**, 135 (1975).
[39] T. Papp, J. Pàlinkàs, L. Sarkadi, B. Schlenk, I. Török, and K. Kiss, Nucl. Instrum. Methods Phys. Res. Sect. B **4**, 311 (1984).
[40] A. Schöler and F. Bell, Z. Phys. A **286**, 163 (1978).
[41] W. Jitschin, H. Kleinpoppen, R. Hippler, and H. O. Lutz, J. Phys. B **12**, 4077 (1979).
[42] W. Jitschin, R. Hippler, R. Shanker, H. Kleinpoppen, R. Schuch, and H. O. Lutz, J. Phys. B **16**, 1417 (1983).
[43] S. Datz, J. L. Duggan, L. C. Feldman, E. Laegsgaard, and J. U. Andersen, Phys. Rev. A **9**, 192 (1974).
[44] J. L. Campbell and J. X. Wang, At. Data Nucl. Data Tables **43**, 281 (1989).
[45] M. O. Krause, J. Phys. Chem. Ref. Data. **8**, 307 (1979).
[46] D. Bhattacharya, G. Kuri, D. P. Mahapatra, M. B. Chatterjee, and P. Sen, Z. Phys. D **28**, 123 (1993).
[47] K. Finck, W. Jitschin, and H. O. Lutz, J. Phys. B **16**, L409 (1983).